Implementation of Quantum Logic Gates by Nuclear Magnetic Resonance Spectroscopy

2000 Chinese Phys. Lett. 17 64

(http://iopscience.iop.org/0256-307X/17/1/022)

Implementation of Quantum Logic Gates by Nuclear Magnetic Resonance Spectroscopy *

DU Jiang-Feng(杜江峰)[1,2], WU Ji-Hui(吴季辉)[2,3], SHI Ming-Jun(石名俊)[1,2], HAN Liang(韩良)[1,2], ZHOU Xian-Yi(周先意)[1,2,4], YE Bang-Jiao(叶邦角)[1,2], WENG Hui-Ming(翁惠民)[1,2], HAN Rong-Dian (韩荣典)[1,2]

[1]*Department of Modern Physics,* [2]*Open Research Laboratory for Quantum Communication and Quantum Computation,* [3]*Laboratory of Structure Biology, University of Science and Technology of China, Hefei 230027*
[4]*International Centre for Materials Physics, Chinese Academy of Sciences, Shenyang 110015*

(Received 4 May 1999)

Using nuclear magnetic resonance techniques with a solution of cytosine molecules, we show an implementation of certain quantum logic gates (including NOT gate, square-root of NOT gate and controlled-NOT gate), which have central importance in quantum computing. In addition, experimental results show that nuclear magnetic resonance spectroscopy can efficiently measure the result of quantum computing without attendant wave-function collapse.

PACS: 89. 70. +c, 03. 65. −w

Quantum computing has a promising future in solving many difficult problems, such as the simulation of quantum systems,[1] and Shor's quantum algorithm of factorization of large numbers. The theory of quantum computing is well understood, but realization of a quantum computer has remained very difficult.[2] Possible methods to implement the quantum computer can be found in systems such as ion traps,[3,4] quantum dots,[5] cavity quantum electrodynamics[6−8] and nuclear magnetic resonance (NMR).[9,10] Only two of these have been successfully used to demonstrate quantum computing so far: ion traps, and NMR. All current approaches to design quantum computers are based on three basic components: quantum bits (qubits), quantum logic gates and read-out of the states.

In our NMR approach, we use a liquid consisting of uniformly deuterated cytosine molecules, whose chemical structure is shown in Fig. 1. The two weakly coupled spin-1/2 hydrogen nuclei, which are distinguished by their different resonance frequencies, i.e. $\omega_A/(2\pi)$ and $\omega_B/(2\pi)$, can be regarded as the isolated qubits. The wave function of the two-qubit state can be generally denoted in the computing basis as

$$\Psi = \sum_{i=0}^{3} c_i|BA\rangle = c_0|00\rangle + c_1|01\rangle + c_2|10\rangle + c_3|11\rangle. \quad (1)$$

Because the energy level differences are small at room temperature and the scalar coupling is weak, the initial state in this two-qubit system is a thermal equilibrium state, which could be approximately denoted as

$$\rho_{\rm eq} = \overline{\rho} + \rho_\Delta = \overline{\rho} + n|00\rangle\langle 00| - n|11\rangle\langle 11| = I_{ZA} + I_{ZB}, \quad (2)$$

where $n \propto \omega_A + \omega_B$ is the proportionality constant, $\overline{\rho}$ is the identity density matrix which gives no effect under a unitary operation, and the usual angular momentum operators in Eq. (2) (such as I_{ZA}, I_{ZB}) are the basic product operators in Liouville space.

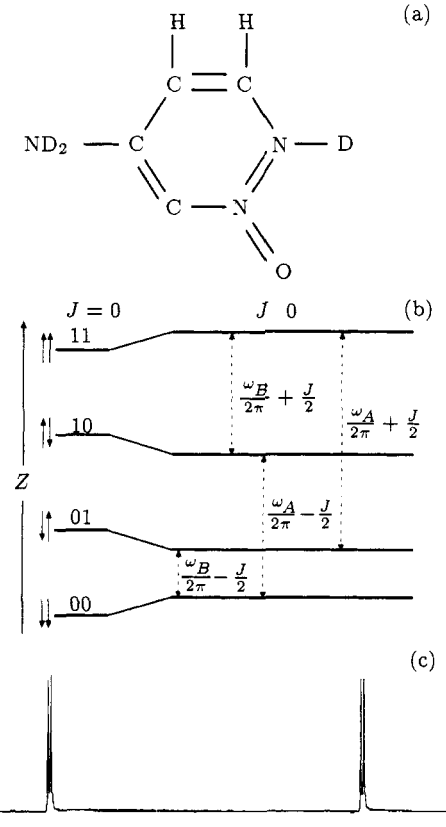

Fig. 1. (a) Chemical structure of deuterated cytosine molecule, the two weakly coupled spin 1/2 hydrogen nuclei denoting the two qubits. (b) Energy level diagram for the two-spin system. (c) NMR spectra obtained by letting a hard readout pulse act on the thermal equilibrium state.

The measured quantity in NMR experiments is the free induction decay (FID) induced in a pick-up coil in the xy-plane: $V(t) \propto \mathrm{i} V_0 T_r \{[\mathrm{e}^{-\mathrm{i}\hat{H}t}\rho(0)\mathrm{e}^{\mathrm{i}\hat{H}t}] \times [(\sigma_x + \mathrm{i}\sigma_y) \otimes I + I \otimes (\sigma_x + \mathrm{i}\sigma_y)]\}$. For example, the schematic spectrum shown in Fig. 1 corresponding of $\rho_{\rm eq}$ of Eq. (2), is acquired from the thermal

*Supported by the National Natural Science Foundation of China under Grant No. 19875050, and the Science Foundation of Chinese Academy of Sciences.

equilibrium state of the sample by applying a hard read-pulse. When the sample is placed in a magnetic field and the coupling term is considered, the four energy levels are shown in Fig. 1. The single-quantum transitions allowed by the selection rules of angular momentum are indicated by two-headed arrows, which connect each pair of states between which only single spin flips exist (noting the spin order is BA). A hard readout pulse applied to the equilibrium state can cause phase procession and generate a detectable (macroscopic) rotating magnetic moment. The real part of the Fourier transform of the resulting signal gives an NMR spectrum containing four peaks at frequencies $\omega_B/(2\pi) + J/2$, $\omega_B/(2\pi) - J/2$, $\omega_A/(2\pi) + J/2$, and $\omega_A/(2\pi) - J/2$. Every pair of lines on the left hand arises from the qubit B, while the pairs of lines on the right hand correspond to the qubit A. The intensity of each pair is proportional to the total population difference between the corresponding states, which results from the following transitions: $|0\rangle(|0\rangle \leftrightarrow |1\rangle), |1\rangle(|0\rangle \leftrightarrow |1\rangle), (|0\rangle \leftrightarrow |1\rangle)|0\rangle$, and $(|0\rangle \leftrightarrow |1\rangle)|1\rangle$. The absolute phase of an NMR signal depends on various complicated experimental details. Therefore, it is difficult to interpret absolute phases. However, using a reference signal can solve this problem. The same phase correction is then applied to the other signal. So from the position, relative phase, intensity and the readout pulse, we can get the state of the sample before the readout pulse. Furthermore, in NMR, instead of a random eigenvalue, the result of a measurement is the expectation value of an observable of the macroscopic ensemble of quantum spins. This implies that nuclear magnetic resonance spectroscopy can efficiently readout the result of quantum computing without attendant wave-function collapse.

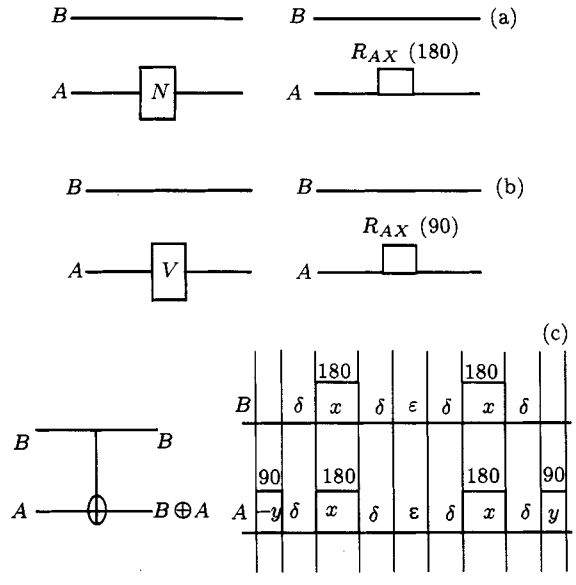

Fig. 2. (a) Quantum circuit symbol for NOT gate (left) and NMR implementation of NOT gate with pulse $R_{AX}(180)$ (right). (b) Quantum circuit symbol for the square-root of NOT gate (left) and NMR implementation of the square-root of NOT gate with pulse $R_{AX}(90)$ (right). (c) Quantum circuit symbol for CNOT gate (up) and NMR implementation of CNOT gate with pulse sequences (down), $\varepsilon = 3\pi/\omega, \varepsilon + 4\delta = 1/2(2J)$.

It was shown that the two-qubit quantum controlled-NOT (CNOT) gate in combination with the set of one-qubit rotations can provide all the quantum logic gates.[11,12] Here are some fundamental quantum logic gates:

$$\begin{aligned} I &\equiv |0\rangle\langle 0| + |1\rangle\langle 1| = \text{identity gate},\\ X &\equiv |0\rangle\langle 1| + |1\rangle\langle 0| = \text{NOT gate},\\ V &\equiv \frac{1}{\sqrt{2}}[|0\rangle(\langle 0| - \mathrm{i}\langle 1|) + |1\rangle(|0\rangle + \mathrm{i}\langle 1|)]\\ &= \text{square} - \text{root of NOT},\\ U_{\text{CNOT}} &\equiv |0\rangle\langle 0| \otimes I + |1\rangle\langle 1| \otimes X\\ &= |00\rangle\langle 00| + |01\rangle\langle 01| + |10\rangle\langle 11| + |11\rangle\langle 10|\\ &= \text{CNOT gate}, \end{aligned}$$

The qubit remains unchanged after the identity gate acting on it. The square-root of NOT gate V can produce the superposition states $|0\rangle \to (1/\sqrt{2})(|0\rangle - \mathrm{i}|1\rangle), |1\rangle \to (1/\sqrt{2})(|0\rangle + \mathrm{i}|1\rangle)$. The NOT gate gives the rotation $|0\rangle \to |1\rangle, |1\rangle \to |0\rangle$. The CNOT gate applies a NOT gate to the target-spin A when the control-spin B is $|1\rangle$ and applies the identity gate to the target-spin A when the control-spin B is $|0\rangle$.

To implement these quantum logic gates in our two-qubit system, we define three gates (U_1, U_2, and U_3) and implement them by using pulse sequences shown in Fig. 2. Since the pulses are much shorter compared to other relevant time scales, other changes of the system during the pulses are ignored. When applying these quantum logic gates to the thermal state, we can calculate the output from $\rho_i = U_i \rho_{\text{eq}} U_i^+$, that is

(1) $U_1 = |00\rangle\langle 01| + |01\rangle\langle 00| + |10\rangle\langle 11| + |11\rangle\langle 10|$, i.e. applying X (NOT gate) to qubit A with qubit B unchanging. U_1 can be implemented by a selected $R_{AX}(180)$ rotation shown in Fig. 2(a).

$$\begin{aligned} \rho_{\text{eq}} \xrightarrow{U_1} \rho_1 &= \overline{\rho} + n|01\rangle\langle 01| - n|10\rangle\langle 10|\\ &= -I_{ZA} + I_{ZB}, \end{aligned} \tag{3}$$

$$\begin{aligned} (2)\ U_2 = \frac{1}{\sqrt{2}}&[|00\rangle(\langle 00| - \mathrm{i}\langle 01|) + |10\rangle(\langle 10| - \mathrm{i}\langle 11|)\\ &+ |01\rangle(\langle 00| + \mathrm{i}\langle 01|) + |11\rangle(\langle 10| + \mathrm{i}\langle 11|)], \end{aligned}$$

i.e. applying the square-root of NOT gate to qubit A. U_2 can be implemented by a selected $R_{AX}(90)$ rotation shown in Fig. 2(b).

$$\begin{aligned} \rho_{\text{eq}} \xrightarrow{U_2} \rho_2 = \overline{\rho} + \frac{ni}{2}&[|00\rangle\langle 01| - |01\rangle\langle 00| + |10\rangle\langle 11|\\ &- |11\rangle\langle 10|] + \frac{n}{2}[|00\rangle\langle 00||01\rangle\langle 01|\\ &- |10\rangle\langle 10| - |11\rangle\langle 11|] = -I_{YA} + I_{ZB}, \end{aligned} \tag{4}$$

(3) $U_3 = |00\rangle\langle 00| + |01\rangle\langle 01| + |10\rangle\langle 11| + |11\rangle\langle 10|$. This is a CNOT gate, implemented by an rf pulse se-

quence in Fig. 2(c).

$$\rho_{\rm eq} \xrightarrow{U_3} \rho_3 = \overline{\rho} + n|00\rangle\langle 00| - n|10\rangle\langle 10| = 2I_{ZA}I_{ZB} + I_{ZB}, \quad (5)$$

where $\sum_{i,j=0}^{3} c_{ij}|i\rangle\langle j|$ is the density operator in Hibert space, and the usual angular momentum operators (such as $I_{\rm ZA}$) in Eq. (3)−(5) are the basic product operators in Liouville space. The input and output states can be read out by letting selective readout pulses $R_{AX}(90)$ act on the target spin A, their schematic NMR spectra are shown in Fig. 3.

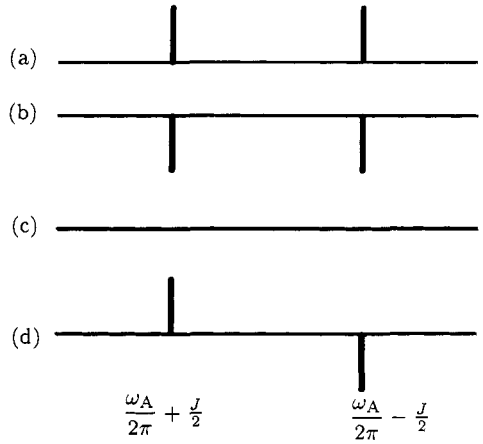

Fig. 3. Schematic NMR spectra obtained by letting a selective readout pulse act on the qubit A: (a) the input thermal equilibrium state $\rho_{\rm eq}$; (b) the output value ρ_3 obyained by U_1 acting on $\rho_{\rm eq}$; (c) the output value ρ_2 obtained by U_2 acting on $\rho_{\rm eq}$; (d) the output value ρ_3 obtained by U_3 acting on $\rho_{\rm eq}$.

All the NMR experiments are conducted at room temperature and pressure on a Bruker Avance DMX-500 spectrometer in the Laboratory of Structure Biology, University of Science and Technology of China. For the two qubits, we choose the two spin 1/2 hydrogen nuclei in the deuterated cytosine molecules. From a fixed input thermal state, we obtained four experimental spectra of the target spin-A by a selective readout pulse $R_{AX}(90)$, expressed as output states $\rho_{\rm eq}$, ρ_1, ρ_2, and ρ_3 appearing in Eqs. (2)−(5). The result is shown in Fig. 4. In our experiment, the frequency difference of the two spins is 765 Hz and the J coupling constant is 7.17 Hz. The transmitter frequency is set in the center of the spectrum, so in the rotating frame $\Delta\omega_B/(2\pi) = -\Delta\omega_A/(2\pi) = 382.5$ Hz, and $\varepsilon = 3\pi/\omega, \varepsilon + 4\delta = 1/(2J)$. Selective excitation on target-spin A was achieved by using Gaussian soft pulses. During a selective pulse the control-spin B (unexcited) continues to experience the main Zeeman interaction, resulting in a rotation around the z-axis, but the length of the selective pulses can be so chosen that the net rotation is almost inexperienced by other spin. It is clear that our implementation of the quantum logic gate leaves the computer in the final result, as expected in Fig. 3. We can see small but significant distortions in the final spectra, due to the difficulty of implementing perfect selective pulses.

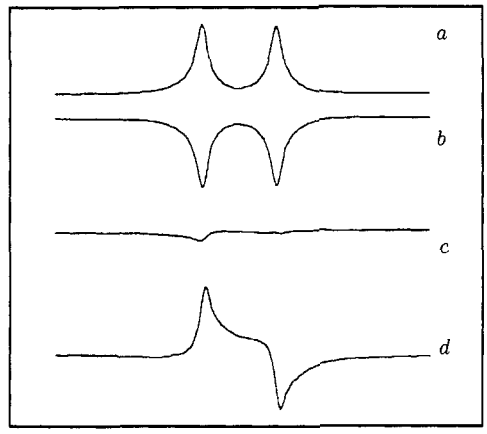

Fig. 4. Experimental NMR spectra obtained by letting a selective readout pulse act on the qubit A: (a) the input thermal equilibrium state $\rho_{\rm eq}$, (b) the output value ρ_1 obtained by U_1 acting on $\rho_{\rm eq}$, (c) the output value ρ_2 obtained by U_2 acting on $\rho_{\rm eq}$, (d) the output value ρ_3 obtained by U_3 acting on $\rho_{\rm eq}$.

In conclusion, with the NMR approach, we have recently demonstrated that the basic quantum logic gates, as well as the state of the system, can be efficiently determined from the NMR spectra collected with suitable read-out pulses. Under the conditions of current schemes, NMR quantum computers will not be able to exceed roughly 10 qubits. But the fact itself can help us study the principles of quantum computation experimentally. It can also help us find the possibility of circumventing this limitation so that large-scale quantum computers can be built.

REFERENCES

[1] R. P. Feynman, Int. J. Theor. Phys. 21 (1982) 467.
[2] P. Shor, in *Proceedings of the 35 th Annual Symposium on Foundations of Computer Science, 1994*, Los Alamitos, California (IEEE Computer Society Press, New York, 1994), p 124.
[3] J. I. Cirac and P. Zoller, Phys. Rev. Lett. 74 (1995) 4091.
[4] C. Monroe *et al.*, Rev. Lett. 75 (1995) 4714.
[5] I. L. Chuang and Y. Yamamoto, Phys. Rev. A 52 (1995) 3489.
[6] Q. A. Turchette *et al.*, Phys. Rev. Lett. 75 (1995) 4710.
[7] S. Bandyopadhyay and V. Roychowdhury, Jpn. J. Appl. Phys. 35 (1996) 3350.
[8] P. Domokos, J. Raimond, M. Brune and S. Haroche, Phys. Rev. Lett. 52 (1995) 3554.
[9] N. A. Gershenfeld and I. L. Chuang, Science, 275 (1997) 350.
[10] J. A. Jones and M. Mosca, J. Chem. Phys. 109 (1998) 1648.
[11] D. P. DiVincenzo, Phys. Rev. A 51 (1995) 1015.
[12] D. Deutsch, A. Barenco and A. Ekert, Proc. R. Soc. London Ser. A 449 (1995) 669.